Physica A 511 (2018) 27–39

Contents lists available at ScienceDirect

Physica A

journal homepage: www.elsevier.com/locate/physa

Discriminating imagined and non-imagined tasks in the motor cortex area: Entropy-complexity plane with a wavelet decomposition

Roman Baravalle [a,b], Osvaldo A. Rosso [c,d,e], Fernando Montani [a,b,*]

[a] IFLYSIB, CONICET & Universidad Nacional de La Plata, Calle 59-789, (1900) La Plata, Argentina
[b] Departamento de Física, Facultad de Ciencias Exactas, Universidad Nacional de La Plata, Calle 49 y 115. C.C. 67, (1900) La Plata, Argentina
[c] Departamento de Informática en Salud, Hospital Italiano de Buenos Aires & CONICET, C1199ABB Ciudad Autónoma de Buenos Aires, Argentina
[d] Instituto de Física, Universidade Federal de Alagoas (UFAL), 57072-900, Maceió, Brazil
[e] Complex Systems Group, Facultad de Ingeniería y Ciencias Aplicadas, Universidad de los Andes, Avenida Monseñor Álvaro del Portillo 12.455, Las Condes, Santiago, Chile

HIGHLIGHTS

- We consider EEG signals of realized and imagined movements.
- We need to infer the dynamical properties of both tasks.
- We use an information theory framework in combination with a wavelet decomposition.
- Entropy-complexity plane allows distinguishing realized from imagined tasks.

ARTICLE INFO

Article history:
Received 19 February 2018
Received in revised form 18 July 2018
Available online xxxx

Keywords:
EEG
Wavelet decomposition
Motor cortex
Motor and imagined movement tasks
Entropy
Complexity

ABSTRACT

Electroencephalograms reflect the electrical activity of the brain, which can be considered ruled by a chaotic nonlinear dynamics. We consider human electroencephalogram recordings during different motor type activities, and when imagining that they perform this activity. We characterize the different dynamics of the cortex according to distinct motor and imagined movement tasks using an information theory approach and a wavelet decomposition. More specifically, we use the entropy-complexity plane $H \times C$ in combination with the wavelet decomposition to precisely quantify the dynamics of the neuronal activity showing that the current theoretical framework allows us to distinguish realized and imagined tasks within the cortex.

1. Introduction

Electroencephalography (EEG) is the physiological method that allow us to measure the electrical activity generated by the brain on the scalp surface. The EEG shows characteristics of the brain activity itself and provides insights of the underlying neural dynamics, and importantly synchronous neuronal discharges generates rhythmic fluctuations that can be also recorded from the scalp using this technique [1–7].

* Corresponding author at: IFLYSIB, CONICET & Universidad Nacional de La Plata, Calle 59-789, (1900) La Plata, Argentina.
E-mail address: fmontani@gmail.com (F. Montani).

https://doi.org/10.1016/j.physa.2018.07.038
0378-4371/

The brain–computer interface (BCI) is a sort of "cooperation" between a brain and a computer device that allows signals from the brain to drive a given external activity, such as control a prosthesis or a cursor [8,9]. This interface permits managing communications between the brain and the object to be commanded. In particular EEG recordings can monitor the cortical activity allowing an EEG-based BCI system to directly control physical or virtual robots and machines [10]. However, not much is known about how a BCI signal processing have to be done in order to decode a message from the brain. The best guidance comes from observations such as EEG signal of imagined movements [11]. If particular imagined hand movements have detectable effects on particular brain signals, we can take advantage of these phenomena as one is therefore able to communicate simple messages using imagery of hand movements [11]. Thus is very important to decode and distinguish the EEG brain signals of real motor movements from imagined movement tasks, classifying the different signal patterns produced by imagined movements [11].

Several methods of EEG analysis are based on the hypothesis that information processing in the brain is reflected in the EEG as dynamic changes of electrical activity in time, frequency and space. Different methodologies have been used to understand the mechanisms behind information processing [12–18]. Among those there also are methods of frequency analysis like Wavelet Transform (WT) which distinguish itself from others due to the high efficiency when dealing with feature extraction. The processing of information in the brain results in dynamic changes in its electrical activity through three variables: time, frequency and space. The "wavelet analysis" is the appropriate mathematical tool to analyze signal in both time and frequency domain [13–15,19]. More specifically, WT allows us to capture fine subtle changes in the EEG signal.

WT was developed as an alternative signal processing technique that allows us to overcome the deficiencies of the Fourier transform and provides a smooth representation, unlike windowed representation in the short time Fourier transform [13,14,19–21]. WT is used for feature extraction and can capture meticulous details like sudden changes and similarities, allowing the preprocessing/denoising of the signal [13,14,19–21]. Importantly, the wavelet transform does not require stationarity, and the time evolution of the frequency patterns can be followed with an excellent time-frequency resolution. The advantages of the WT are particularly important when analyzing EEGs as the definition of spectral entropies is based on the distribution of the activity in the frequency domain allowing us to analyze EEG signals at different scales. The wavelet time-frequency representation does not make any assumptions about stationarity of the signal and is capable of detecting dynamic changes due to its localization properties. Wavelets are well localized in both time and frequency, and the computational time is short since the algorithm involves the use of fast wavelet transform in a multi-resolution framework. Importantly, contaminating noise contributions can be easily eliminated when they are concentrated in any frequency bands. WT can provide a time-variant decomposition, which means a significant advantage over filtering techniques, as taking a time-disparity decomposition it allows us to take different wavelet coefficients inducing distinct filtering situations for diverse time windows. That is, WT makes possible to generate event related filter responses.

The main advantage of the wavelets is that they deliver the best relation between frequency resolution and time windowing, reaching the lower limit in the time-frequency uncertainty principle [13]. In addition the wavelet entropy (WE) provides an accurate quantification of the frequency content of the EEG signals and, moreover, is an ideal candidate for measuring how spontaneous oscillations of the ongoing EEG get ordered upon stimulation [13]. This method was successfully applied for studying the ordering of the EEG during grand mal epileptic seizures [19,22]. In this paper we propose a wavelet decomposition of the EEG signal to distinguish motor and imagined movement tasks within the cortex considering a subtle measure accounting for the normalized Shannon entropy (H) [19,21,23,24] and Martín, Plastino, Rosso statistical complexity (C) [19,21,23,24]. Our approach allows us to quantify the dynamic of the signals, inferring the emergent properties of the system through a two dimensional representation $H \times C$, suggesting how brain EEG activity is related to imagined movements and distinguishing real motor movements from imagined ones within the cortex.

2. Methodology

2.1. Information theory measures

2.1.1. Information measures

In the following we use the notation of Ref. [19]. Any information measure I can be defined as a functional that characterizes a given probability distribution $P = \{p_j; j = 1, \ldots, N\}$, with N the number of possible states allowed for the system.

We define for a given discrete probability distribution P and its associate information measure $I[P]$, an amount of disorder H

$$H[P] = I[P]/I_{max}, \tag{1}$$

where $I_{max} = I[P_e]$ and $P_e = \{\frac{1}{N}, \ldots, \frac{1}{N}\}$ is the uniform distribution. Thus, H is a quantity between 0 and 1. In our case we choose I as the Shannon's entropy $S[P] = -\sum_{j=1}^{N} p_j \log(p_j)$. The entropy H would be zero when the knowledge of the system state would be maximal (i.e. only one of the p_j is 1 and the rest are 0). The entropy H is equal to one when the system is likely to be in any state (i.e. P equals the uniform distribution P_e). In both cases, we say that the system is not in a complex state, because it is either in a state of perfect order or disorder.

Thus, in order to quantify the complexity of the system state, we define a quantity named *statistical complexity measure* (SCM). The statistical complexity should be zero for the two extremes: complete order or complete disorder. Before introduce this measure, we define the "disequilibrium" as $Q[P] = Q_0 D[P, P_e]$, where Q_0 is a normalization constant, so $0 \leq Q \leq 1$, and $D[P, P_e]$ is a distance between the probability under study P and the uniform distribution P_e. For the distance D we use the Jensen–Shannon divergence between the system's density function and the uniform distribution: $D = J_S[P, P_e] = S\left[\frac{P+P_e}{2}\right] - \frac{S[P]}{2} - \frac{\log(N)}{2}$.

That is we can take the following definition for the MPR statistical complexity measure [23,24], C:

$$C[P] = H[P]\, Q[P]. \tag{2}$$

This quantity reflects on the interplay between the amounts of information stored in the system and its disequilibrium [19, 21]. This complexity measure satisfies the condition that $C[P] = 0$ when the system is in a very ordered state (this value is obtained when one of the components of P, like p_m, is equal to one and the remaining p_j are equal to zero) or in a very disordered state (when $P = P_e$).

2.1.2. Wavelet transform and wavelet-based information measures

Unlike in Fourier analysis, in which the sine and cosine functions are used, the wavelet transform is based in functions that are vanishing oscillating functions. Within the wavelet multiresolution decomposition framework a wavelet family $\psi_{a,b}$ is a set of elemental functions generated by scaling and translation of a unique admissible mother wavelet $\psi(t)$:

$$\psi_{a,b} = |a|^{-1/2}\, \psi\left(\frac{t-b}{a}\right), \tag{3}$$

where $a, b \in \mathbb{R}$, $a \neq 0$, are the scale and translation parameter, respectively, and t is the time [19].

The continuous wavelet transform (CWT) of a signal $S(t) \in L^2(\mathbb{R})$ (the space of real square summable functions) is defined as the correlation between the signal $S(t)$ with the family wavelet $\psi_{a,b}$ for each a and b:

$$\langle S, \psi_{a,b}\rangle = |a|^{1/2} \int_{-\infty}^{\infty} S(t)\psi^*\left(\frac{t-b}{a}\right) dt \tag{4}$$

where * means complex conjugation. In principle, the CWT gives a highly redundant representation of the signal, because it produces an infinite number of coefficients [19]. A non redundant and efficient representation is given by the discrete wavelet transform (DWT), which also allows to a complete signal reconstruction. For a special election of the mother wavelet function $\psi(t)$ and the discrete set of parameters $a_j = 2^{-j}$ and $b_{j,k} = 2^{-j}k$, with $j, k \in \mathbb{Z}$, the family $\psi_{j,k}(t) = 2^{j/2}\psi(2^j t - k)$ constitutes an orthonormal basis of $L^2(\mathbb{R})$. Any arbitrary function of this space therefore can be uniquely decomposed and the decomposition can be inverted [19]. The wavelets coefficients of the DWT are $\langle S, \psi_{j,k}\rangle = C_j(k)$. The DWT produces only as many coefficients as there are samples within the signal under analysis $S(t)$, without any loss of information.

Let us assume that the signal is given by the equally sampled values $S = \{s_0(n), n = 1, \ldots, M\}$, with M the total number of samples. If the decomposition is carried out over all resolution levels, $N_J = \log(M)$, the wavelet expansion reads:

$$S(t) = \sum_{j=-N_J}^{-1} \sum_{k} C_j(k)\psi_{j,k}(t) = \sum_{j=-N_J}^{-1} r_j(t), \tag{5}$$

where the wavelet coefficients $C_j(k)$ can be interpreted as the local residual errors between successive signal approximations at scales j and $j-1$, respectively, and $r_j(t)$ is the detail signal at scale j, that contains information of the signal $S(t)$ corresponding with the frequencies $2^{j-1}\omega_s \leq |\omega| \leq 2^j\omega_s$, being ω_s the sampling frequency [19,21].

Since the family $\psi_{j,k}(t)$ is an orthonormal basis for $L^2(\mathbb{R})$, the concept of wavelet energy is similar to the Fourier theory energy. Thus, the energy at each resolution level $j = -1, \ldots, -N_J$, will be the energy of the detail signal:

$$E_j = \|r_j\|^2 = \sum_k |C_j(k)|^2. \tag{6}$$

The total energy can be obtained summing over all the resolution levels

$$E_{tot} = \|S\|^2 = \sum_{j=-N_J}^{-1} \sum_k |C_j(k)|^2 = \sum_{j=-N_J}^{-1} E_j. \tag{7}$$

Finally, we define the relative wavelet energy (RWE) through the normalized ρ_j values:

$$\rho_j = \frac{E_j}{E_{tot}} \tag{8}$$

for the resolution levels $j = -1, -2, \ldots, -N_J$. The distribution $P^{(W)} \equiv \{\rho_j\}$ can be viewed as a time-scale distribution which is a suitable tool for detecting and characterizing phenomena in the time and the frequency spaces [19].

Using the definition of Shannon entropy, we can define the Shannon wavelet entropy (SWS) as

$$S\left[P^{(W)}\right] = H\left[P^{(W)}\right] = -\sum_{j=-N_j}^{-1} \rho_j \log\left(\rho_j\right), \tag{9}$$

where $P^{(W)}$ denotes the probability energy wavelet distribution. As mentioned early, the SWS is a measure of the degree of order/disorder of the signal, providing information about the underlying dynamical process associated with the signal.

Taking into account the definition of the SCM in Eq. (2), and using the energy wavelet distribution $P^{(W)}$ and the corresponding equiprobability wavelet distribution $P_e^{(W)} = \{\frac{1}{N_j}, \ldots, \frac{1}{N_j}\}$, we can evaluate the disorder $H\left[P^{(W)}\right]$ and the disequilibrium $Q\left[P^{(W)}\right]$, in order to obtain the wavelet SCM as:

$$C\left[P^{(W)}\right] = H\left[P^{(W)}\right] Q\left[P^{(W)}\right]. \tag{10}$$

In the following section we describe the experimental methodology of the EEG recordings that will be used to test our current approach.

2.2. Experimental methods

We have considered the EEG Motor Movement/Imagery Dataset recorded using BCI2000 [11] instrumentation system available through Physionet [25–28]. The dataset consists of more than 1500 EEG recordings, with different durations (one or two minutes per record), obtained from 109 healthy subjects. The 109-subjects data on Physionet is screening data in which the subjects had to perform one movement or imagery task at a time. The population of volunteers was drawn from the employer at the New York State Department of Health, i.e, all the subjects had completed high school training and most of them had completed four years of College education. The sex and age of the subjects have not been reported as relevant for performing these tasks. All subjects were naive. As learning proceeded with further repetitions of the experiment, imagery usually became less important and performance becomes more automatic [25–30]. Subjects were asked to perform different motor/imagery tasks while EEG signals were recorded from 64 electrodes along the surface of the scalp. Each subject performed 14 experimental runs:

- A one-minute baseline runs (with eyes open)
- A one-minute baseline runs (with eyes closed)
- Three two-minute runs of each of the four following tasks:

(1) A target appears on either the left or the right side of the screen. The subject opens and closes the corresponding fist until the target disappears. Then the subject relaxes.
(2) A target appears on either the left or the right side of the screen. The subject imagines opening and closing the corresponding fist until the target disappears. Then the subject relaxes.
(3) A target appears on either the top or the bottom of the screen. The subject opens and closes either both fists (if the target is on top) or both feet (if the target is on the bottom) until the target disappears. Then the subject relaxes.
(4) A target appears on either the top or the bottom of the screen. The subject imagines opening and closing either both fists (if the target is on top) or both feet (if the target is on the bottom) until the target disappears. Then the subject relaxes.

The 64-channels EEG signals were recorded according to the international 10–20 system (as seen in Fig. 1). The sampling frequency of the EEG is 160 Hz. The order of the recordings are: Baseline with open eyes, Baseline with closed eyes, and then Task 1, Task 2, Task 3 and Task 4 successively until the 14 runs where completed. The right mastoid bone corresponds to ground (GND) and the right earlobe to reference (REF) [25,27–30]. The impedance was kept under 10 kΩ. The data are raw data without any re-referencing. There was no EOG recording. The data are raw without any post-processing. A variety of sensors for monitoring brain activity were used. Muscular artifacts (electromyographic (EMG) signals) were carefully checked at the beginning of each recording, and verified throughout the recording. During the recordings light was dimmed, and the experiment was performed in a closed room where the external sounds were minimized. As the learning proceeds, imagery usually becomes less important [25–30]. The timing from the event markers was of 1 s and they are stated in the dataset (see Ref. [28]), the tasks order was block-randomized, in blocks of 8. For further details of the EEG data acquisition we refer the reader to Refs. [25,27–30].

For each subject and for each task we perform an average of the signals, resulting in ERPs associated with each task. In this paper, we consider the recordings which have the same number of stimuli of each type, resulting in just 87 subjects (of the 109-subjects data mentioned above). That is we consider 87 subjects for whom the number of stimuli presented, and the duration of each stimulus-rest interval was exactly the same. Then we choose 87 subjects with exactly the same stimulation protocol. In addition, the order of presentation of the stimuli for each of subject this 87 subjects in each run is also identical (stimulus-rest-stimulus-rest).

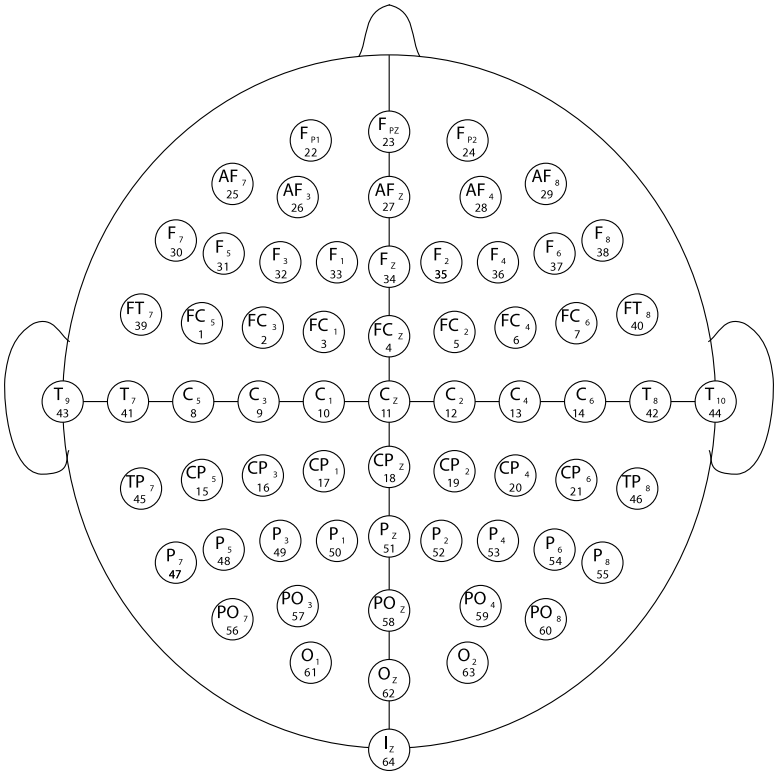

Fig. 1. Electrode arrangement as per the international 10–20 system (as in [11,27–30]). The numbers below each electrode name indicate the order in which they appear in the recordings.

3. Results

EEG is the recording of intrinsic electrical activity in the brain and it is based on the propagation of electric impulses along a nerve fiber when the neuron fires. The experimental setup of the BCI2000 system is shown in Fig. 1, and consist of an arrangement of the different used electrodes [25,27–30]. Eye blink artifacts are generated by fast movements of the eyelid along the cornea, such as during an eye blink. Muscular artifacts were carefully checked at the beginning of each recording, and verified throughout the recording [25,27–30]. In our current analysis the muscular and technical artifacts of the EEG Motor Movement/Imagery Dataset were removed following the methodology, similar to the one presented in [11], which is indicated below:

(1) A Common Average Reference (CAR) filter is performed. A spatial high-pass filter, is implemented by re-referencing the potential $s_h(t)$ of each electrode h at each time point t to an estimated reference that is calculated by averaging the signals from all H recorded electrodes. In other words, a CAR filter calculates the signal amplitude that is common to all electrodes $\frac{1}{H}\sum_{i=1}^{H} s_i(t)$ and subtracts it from the signal $s_h(t)$ at each location.
(2) We applied the Kaiser filtering of 60 dB of attenuation, between 1 Hz and 50 Hz (see Ref. [31])
(3) Selecting Epochs.
(4) Baseline corrects was set ranging from 100 ms before the onset of each stimulus presentation to analyze Event Related Potentials (ERPs).
(5) Averaging the event-related potentials (ERPs).
(6) Rejection of artifacts. That is we just compare the obtained signal using the previous steps with the one acquired using an automatic methodology called wICA [32,33].

By recording small potential changes in the EEG signal immediately after the presentation of a sensory stimulus it is possible to record specific brain responses to specific sensory, cognitive and other mental events. This method is called Event-Related Potentials and is one of the classic methods for investigation of mental states and information processing [13,14]. In this case to analyze the EEG Motor Movement/Imagery Dataset [25,27–30] we consider a duration of the analysis epoch of 1500 ms and a mean number of single trials used for averaging of 21 single trials (there were 7 stimulus presentations for each experimental run, and 3 runs for each stimulus condition). Baseline corrects was set ranging from 100 ms before the onset of each stimulus presentation to analyze ERPs. The onset stimulus is used for averaging (that is, we used the presentation of

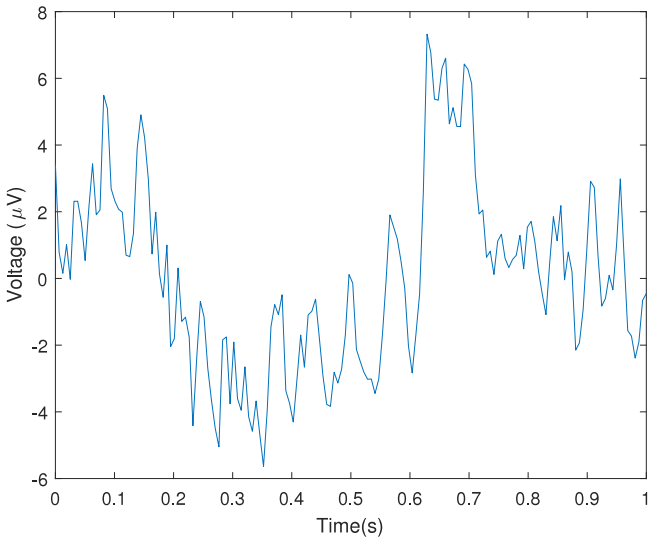

Fig. 2. Raw signal corresponding to electrode FC_5 located over the motor area, during the right hand motor condition.

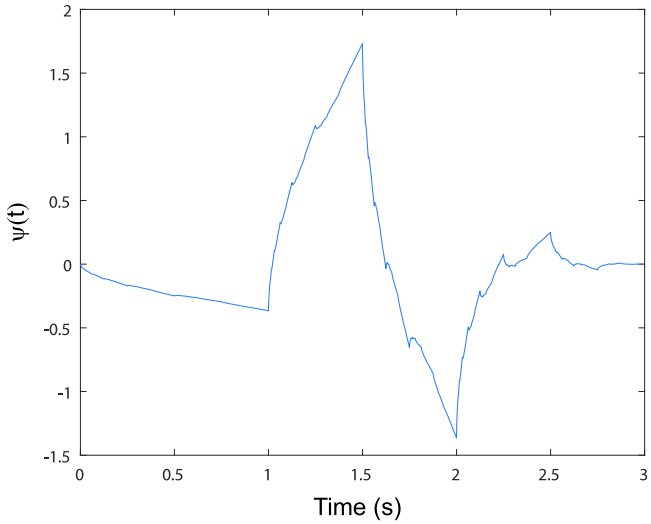

Fig. 3. Daubechies 2 mother wavelet.

the stimulus as a trigger to average). Once we have obtained the distribution of energy for each ERP signal corresponding to one task, we can use the Information Theory quantifiers (of Section 2.1) to describe this energy distribution.

Fig. 2 depicts a typical raw signal that corresponds to electrode FC_5 during the right hand motor condition. For analyze these signals we use as a mother wavelet the Daubechies 2 [34] that is presented in Fig. 3 (see below for further details). After a 6 octave wavelet decomposition, coefficients were obtained for the following resolution levels (frequency bands): 80–160 Hz ($j = -1$; not used for further analysis); 40–80 Hz ($j = -2$; not used for further analysis); 20–40 Hz ($j = -3$); 10–20 Hz ($j = -4$), 5–10 Hz ($j = -5$) and 2.5–5 Hz ($j = -6$); the residue was in the 1–2.5 Hz band ($r = -6$). The residue was also removed for the analysis.

The EEG are highly nonstationary, but the Fourier transform (FT) requires stationarity of the signal and FT does not give the time evolution of the frequency patterns [19]. In contrast, the orthogonal discrete wavelet transform makes no assumptions about record stationarity and the only input needed is the time series [13,19,21,22,35–39]. In this case, the time evolution of frequency patterns can be followed with an optimal time-frequency resolution. The wavelet multiresolution decomposition, described in Section 2.1.2, is used to split the signals in scale levels used by the clinical EEG analysis [19,21,35–38]. In particular Daubechies proposed a discrete, maximally flat, compactly supported, orthogonal wavelet family known as the Daubechies wavelets [34]. This wavelet family is important for signal processing applications [40]. The Daubechies wavelets (DB wavelet) are the most commonly used wavelets as they provide better performance in localizing characteristics of the

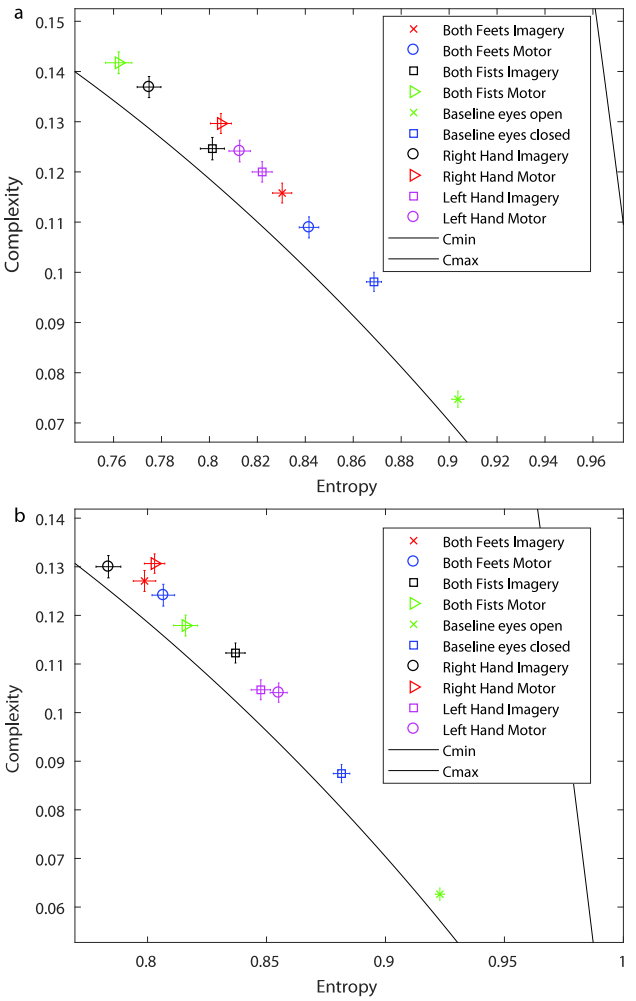

Fig. 4. Entropy-complexity plane considering the mean between all subjects for electrodes: (a) FC_3 and (b) PO_7. We consider movement or imagery tasks, and the baselines with open and closed eyes. The solid black lines correspond to maximum C_{max} and the minimum C_{min} values of the complexity.

signal. In particular the Daubechies 2 (DB2) wavelet permits to successfully locate changes in the wave shape at faulty points enhancing specific features of a signal (Fig. 3 shows the DB2 mother wavelet). A few preliminary tests allows us to find that the DB2 to provide a better discrimination than DB4 between pure motor and imagined movement. Thus we choose the DB2 to perform the analysis over the 64 electrodes. We applied the wavelet DB2 between 2.5 Hz and 40 Hz.

Fig. 4 displays, for all the 87 subjects here considered, the entropy-complexity plane $H \times C$ location. More specifically, we analyzed the entropy-complexity plane, $H \times C$, for a central motor electrode FC_3 and (b) PO_7. This figure depicts that the entropy-complexity plane $H \times C$ allows us a"robust" distinction between motor and imagined movement tasks, and with respect to the baselines (with open and closed eyes). Note that the baseline epoch with open eyes is different from the baseline used for averaging, as it is a long run without any stimulus. Let us remark that we consider two one-minute baseline runs (one with eyes open and one with eyes closed). Although in Fig. 4(b) the left hand imagery and motor depicts similar complexity values, the entropy-complexity plane, $H \times C$, allows a proper distinction between the dynamics of the different tasks. That is the combination of both entropy and complexity that allow us to distinguish imagery from realized movements. Let us emphasize for a given value of H, the range of possible C values varies between a minimum C_{min} and a maximum C_{max} that are depicted by the black solid lines, restricting the possible values of the statistical complexity in a given entropy-complexity plane [41], values that depend only on the number degree of freedom of the considered probability distribution function (PDF). The entropy and complexity are estimated through the distribution of energy for each ERP signal as it is convenient to have a smoother signal to reduce bias deviations from our estimations.

The previous result motivated us to investigate in more detail the $H \times C$ planes of the imagery and realized movements for other electrodes over the cortex. Fig. 5(a)–(d) show the $H \times C$ planes of four different subjects and for 64 electrodes along the surface of the scalp, considering the motor and imagery task with the left hand. Fig. 6(a)–(d) depict the $H \times C$ planes

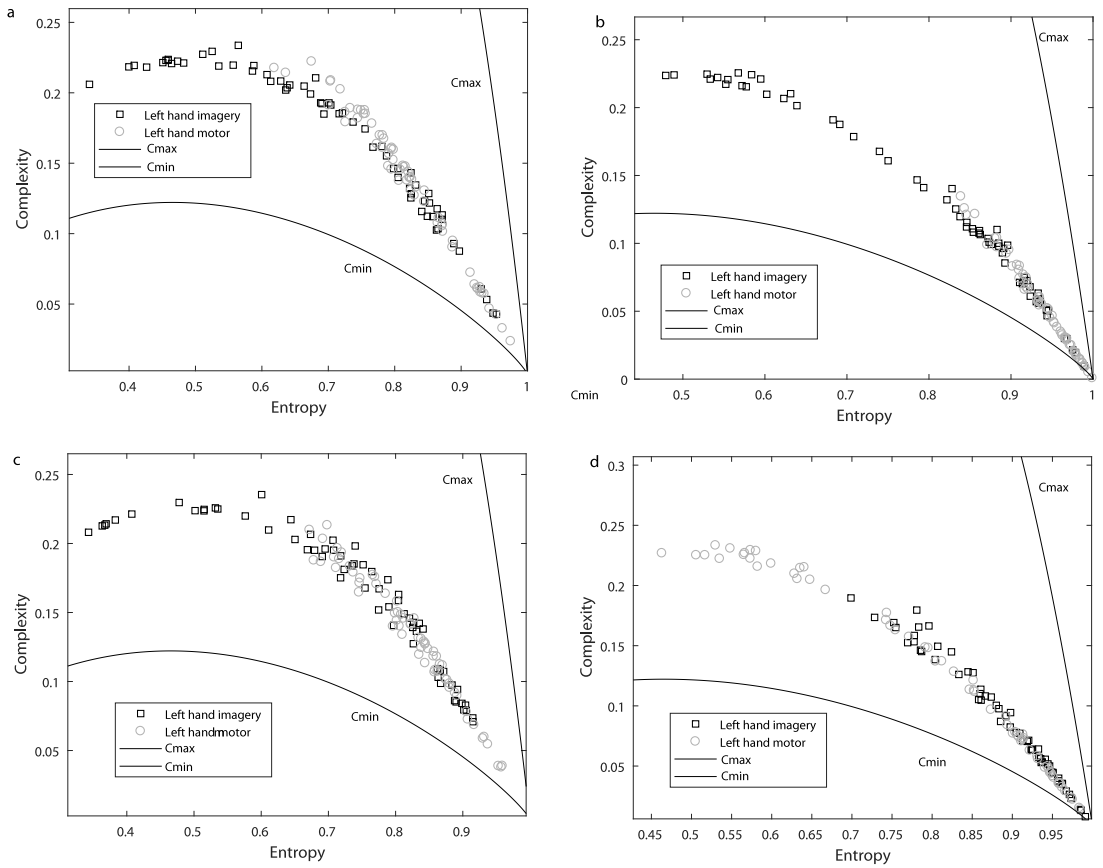

Fig. 5. Entropy-complexity plane for the tasks related with left hand, movement or imagery, taking into account the 64 electrodes. We highlight four different subjects that have different distributions of motor and imagery task with the left hand with at least a 95% confidence: (a) number 11; (b) number 30; (c) number 33; and (d) number 72. The solid black lines correspond to maximum C_{max} and the minimum C_{min} values of the complexity.

considering the motor and imagery task with the right hand for the same 64 electrodes as Fig. 5(a)–(d). We performed a t-test for the distributions depicted in the entropy-complexity plane, $H \times C$, of Figs. 5 and 6. The result for both variables in entropy-complexity plane, $H \times C$, are that 43 of 87 subjects considered here have different distributions between motor and imagery task with the left hand with at least a 95% confidence (the test rejects the null hypothesis at the 5% significance level). Instead in the case $H \times C$ planes considering the motor and imagery task with the right hand for both variables in entropy-complexity plane, $H \times C$, there are 77 of the 87 subjects that have different distributions at least a 95% confidence (the test rejects the null hypothesis at the 5% significance level). The system's localization in an entropy-complexity plane (global quantifier) displays typical specific features associated with its dynamics' nature of the brain. And, we can appreciate that for a very significant, subjects the realized movement with the right hand have a different dynamics in entropy-complexity plane, $H \times C$.

We also investigate the entropy-complexity plane, $H \times C$, in the cases in which both task are just realized movements, taking into account the right and left hand movements for the 64 electrodes, as shown in Fig. 7. The $H \times C$ plane allows to distinguish between the different right and left for realized movements for 42 of 87 subjects considered here as they have different distributions at least a 95% confidence (the t-test rejects the null hypothesis at the 5% significance level). However, we find a significant larger number of subjects with different distributions when considering just the imagery movements, with left or right hand, as shown in Fig. 8. The result for both variables in entropy-complexity plane, $H \times C$, are that 76 of 87 subjects considered here have different distributions with at least a 95% confidence when considering just the imaginary tasks either with the right or left hand (the t-test rejects the null hypothesis at the 5% significance level).

Note that the maximum C_{max} and the minimum C_{min} values of the complexity restrict the possible values of the intensive statistical complexity in the $H \times C$ plane. Localization in the entropy-complexity plane $H \times C$, in some cases, closely approaches the limiting curve of minimum statistical complexity C_{min}. However, even the evaluation of lower values of the complexity provides additional insight into the details of the system's probability distribution, which is not discriminated by randomness measures like the entropy [42,43]. Complexity helps to uncover information related to the correlational structure of the physical process under study. The entropy-complexity diagram (or plane), $H \times C$, allows us to detect subtle

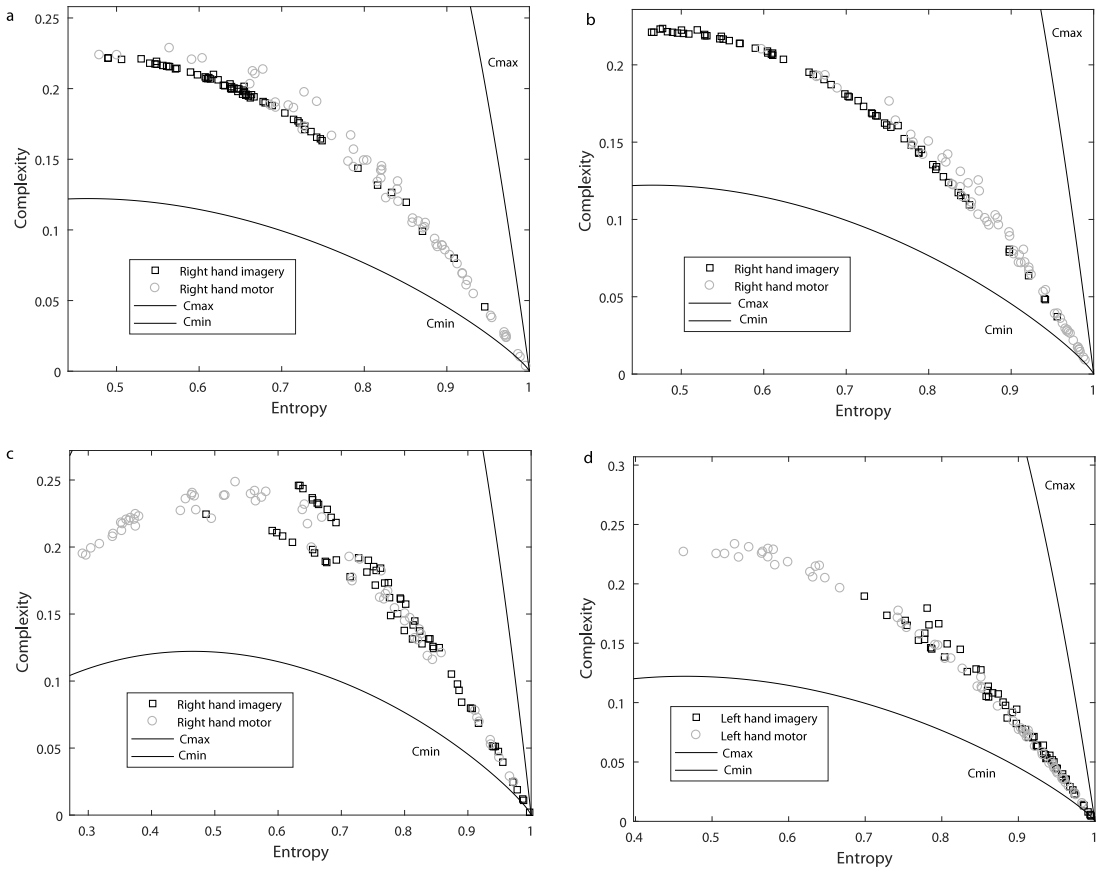

Fig. 6. Entropy-complexity plane for the tasks related with right hand, movement or imagery, taking into account the 64 electrodes. We consider four different subjects: (a) number 11; (b) number 30; (c) number 33; and (d) number 72. The solid black lines correspond to maximum C_{max} and the minimum C_{min} values of the complexity.

changes in the neural dynamics of a system originated by modifications of the external stimuli. This provides a distinction between chaotic-deterministic and stochastic dynamics [23,24,44–47].

The system's localization in an entropy-complexity plane allows us quantify specific features associated with left or right hand for a given specific task. This is the entropy-complexity plane, $H \times C$, is able to detect essential details of the brain dynamics and distinguishing underlying peculiarities of imagery and realized tasks for different groups of subjects. That is, we show that is possible to make a distinction between imagery and realized tasks, using the Information Theory quantifiers described in this work. The Wavelet-MPR-Complexity approach is therefore a suitable candidate for an accurate classification of the different motor activities made by the right/left hand and by imagined tasks.

4. Discussion and conclusions

Complexity captures the degree to which a neuronal system integrates specialized information and, in particular, the complexity of the neural system represents the amount of information contained in the organism, in the sense that it quantifies the dynamic characteristics of the temporal pattern due to the functional interactions produced by a structural network. In particular, the statistical complexity of MPR can distinguish time series generated by stochastic and chaotic systems [23,24]. This measure of statistical complexity can also detect and quantify order induced by noise [23,24]. The development of theoretical tools that could provide new insights into how mind/brain mechanisms work can help to improve our understanding of different cognitive processes. In this paper we show that the combination of the statistical complexity and entropy concepts with wavelet transforms can provide new crucial insights into this problem.

That is, the main objective of our current work is to infer the emergent dynamical properties of the neuronal system through the entropy-complexity plane, $H \times C$. This is to quantify critical details of neural dynamical processes underlying the dataset as measures of statistical or structural complexity are necessary for a better understanding of chaotic time series because they are able to capture their organizational properties [23,24,44–47]. This specific kind of information is not revealed by randomness' measures. Perfect order (like that of a periodic sequence) and maximal randomness (fair coin

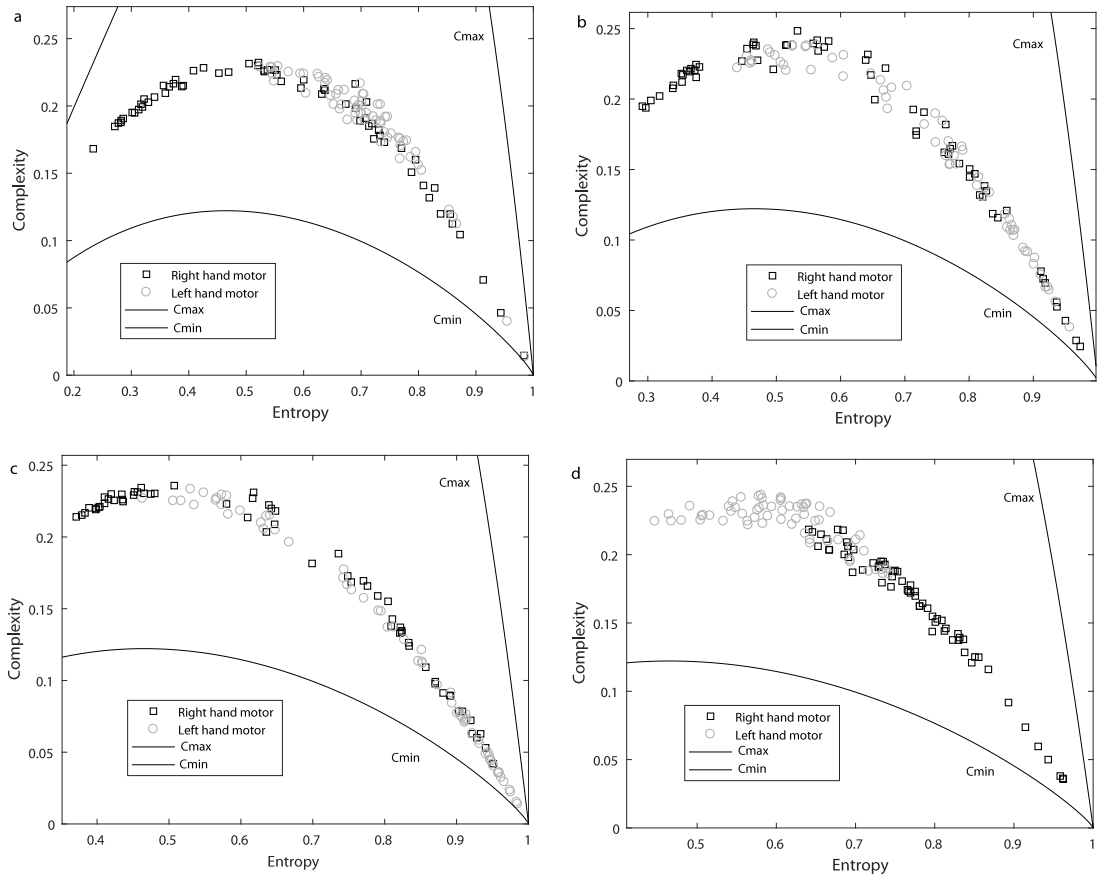

Fig. 7. Entropy-complexity plane for the tasks related with movement, left or right hand, taking into account the 64 electrodes. We consider four different subjects: (a) number 11; (b) number 30; (c) number 33; and (d) number 72. The solid black lines correspond to maximum C_{max} and the minimum C_{min} values of the complexity.

toss) possess no complex structure and exhibit zero statistical complexity. For states between these extremes a wide range of possible degrees of structure exists, that should be quantified by an appropriate statistical complexity measure. The Jensen–Shannon divergence, that quantifies the difference between two (or more) probability distributions, is especially useful to compare the symbol-composition of different sequences. The complexity measures constructed in this way has the intensive property found in many thermodynamic quantities [23,24,44–47]. We stress the fact that the statistical complexity is the product of a normalized entropies and a statistical distance between distributions (the Shannon entropy and Jensen–Shannon divergence) and it is a nontrivial function as it depends on two different probabilities distributions, i.e., the one corresponding to the state of the system, P, and the uniform distribution, P_e, taken as reference state. The statistical complexity measure used here is able to (i) detect essential details of the dynamics and (ii) differentiate between chaos and (different degrees of) periodicity [23,24].

Thus complexity provides important additional information regarding the peculiarities of the underlying PDF, that is not detected by the entropy. We found that the $H \times C$ plane allows us to distinguish particularly well the right handed movement from the imagined ones. We are also able to distinguish the pure imagined movement between both hands. This effect is lower when distinguishing left handed movements from realized ones. We have chosen the DB2 to perform the analysis over the 64 electrodes. However, some positions of the frontal cortex showed more variability with respect to other areas, and therefore for future related works we plan to use a different wavelet for the frontal area like for instance the Morlet [48,49] and the DB2 for the rest of the electrodes. This can be helpful to improve the estimations performed using the entropy-complexity plane, $H \times C$, and these small adjustments will make the current methodology even more efficient. Notice that is the combination of both entropy and complexity depicted the plane, $H \times C$, that allow us to distinguish imagery from realized movements. In other words entropy and complexity are different concepts that are complementary to each other. Summarizing, the system's localization in an entropy-complexity plane ($H \times C$) provides a global quantifier that displays typical specific features associated with its dynamics' nature of the realized and imagined movements.

We investigate then the entropy-complexity plane $H \times C$ considering a wavelet decomposition of the EEG signal to distinguish motor and imagined tasks over the motor cortex. This allows us to characterize the internal dynamics of

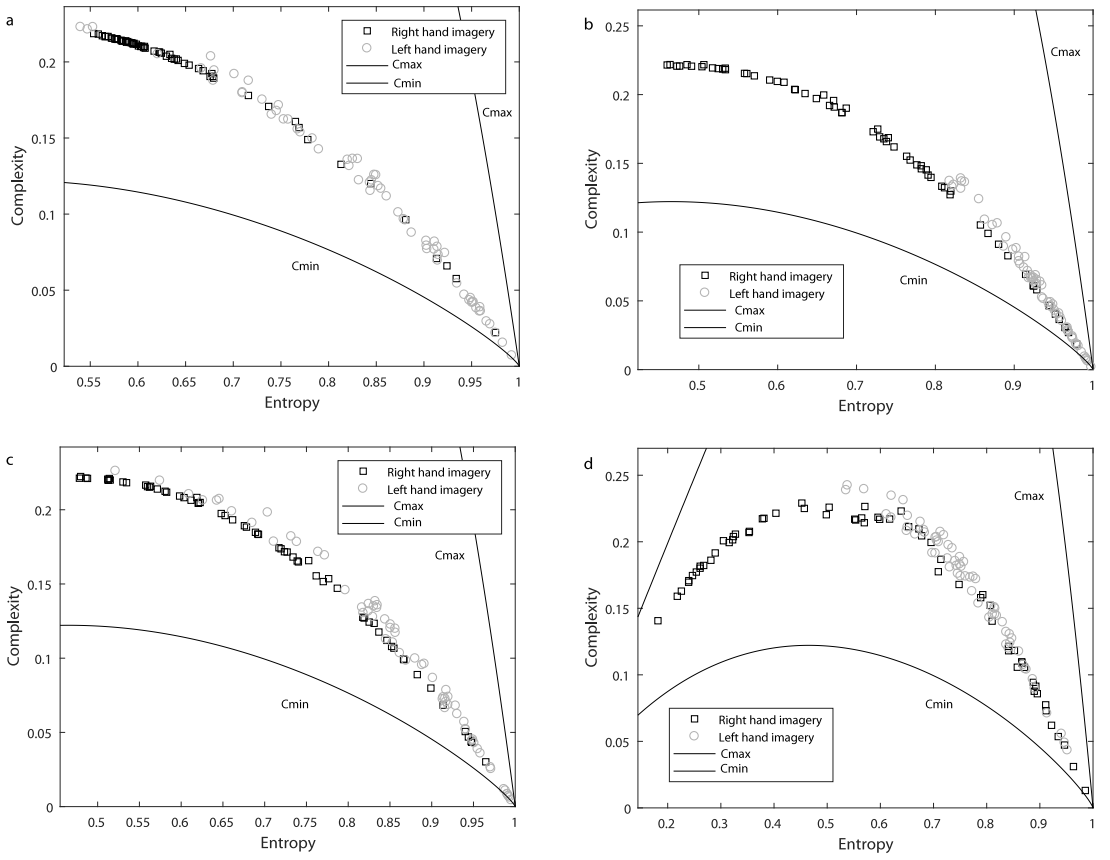

Fig. 8. Entropy-complexity plane for the tasks related with imagery, left or right hand, taking into account the 64 electrodes. We consider four different subjects: (a) number 11; (b) number 30; (c) number 33; and (d) number 72. The solid black lines correspond to maximum C_{max} and the minimum C_{min} values of the complexity.

the neural system when taking into account the imagined and non-imagined tasks. We show that using the wavelet decomposition in combination with recent advances in statistical complexity measures ($H \times C$ plane) is physiologically meaningful since it helped us to distinguish a motor specific neurophysiological state with the imagined one. Moreover, our approach allows us to identify the different dynamics when considering the signal of the right and left hand, and also making possible to distinguish between imagery and realized tasks, quantifying the nonlinearities of the signal, and inferring the emergent properties of the system over the cortex.

The information plane $H \times C$ can be used profitably to separate and differentiate between chaotic and deterministic systems [50]; visualization and characterization of different dynamic regimes when the system parameters vary [50–52]; dynamic evolution of time [53]; identifying periodicities in natural time series [54]; identification of deterministic dynamics contaminated with noise [55,56] and intrinsic estimation time scales of delayed systems [57,58]; among other applications [59]. Importantly in this paper, we show that the motor task and imagined activities can be associated with different complex dynamic reflected in the entropy-complexity plane, $H \times C$, allowing us to quantify the dissimilarities between both within the motor cortex area. That is the entropy-complexity plane, $H \times C$, with a wavelet decomposition can serve as the basis for a successful BCI [8,9], a technology that can help people who are severely disabled. Thus by identifying the meaningful signal information of the EEG signal within the plane $H \times C$ with a wavelet decomposition we can provide a mapping of human imagined motor activities that could be decoded into certain movements of artificial actuators. Decoding properly the imagined task from the realized ones can help us to understand how to communicate subtle artificial movement of an external device.

Acknowledgments

We gratefully acknowledge funding from PIP 11220130100327CO (2014/2016) CONICET, Argentina (F.M.) and Universidad Nacional de La Plata, Argentina (project 11/X812).

References

[1] A. Kostov, M. Polak, Parallel man-machine training in development of EEG-based cursor control, IEEE Trans. Rehabil. Eng. 8 (2000) 203–205.
[2] J.R. Wolpaw, D.J. McFarland, G.W. Neat C.A. Forneris, An EEG-based brain-computer interface for cursor control, Electroencephalogr. Clin. Neurophysiol. 78 (1991) 252–259.
[3] J.R. Wolpaw, D.J. McFarland, Multichannel EEG-based brain-computer communication, Electroencephalogr. Clin. Neurophysiol. 90 (1994) 444–449.
[4] J.R. Wolpaw, D.J. McFarland, Control of a two-dimensional movement signal by a noninvasive brain-computer interface in humans, Proc. Natl. Acad. Sci. USA 101 (2004) 17849–17854.
[5] D.J. McFarland, G.W. Neat, R.F. Read, J.R. Wolpaw, An EEG-based method for graded cursor control, Psychobiol. 21 (1993) 77–81.
[6] J. Millán, F. Renkens, J. Mourino, W. Gerstner, Noninvasive brain-actuated control of a mobile robot by human EEG, IEEE Trans. Biomed. Eng. 51 (2004) 1026–1033.
[7] G. Pfurtscheller, D. Flotzinger, J. Kalcher, Brain-computer interface: a new communication device for handicapped persons, J. Microcomput. Appl. 16 (1993) 293–299.
[8] E. Leuthard, G. Schalk, J.W. Ojemann, D. Moran, A brain-computer interface using electrocorticographic signals in humans, J. Neural Eng. 1 (2004) 63–71.
[9] J. Wilson, E. Felton, P. Garell, G. Schalk, J. Williams, ECoG factors underlying multimodal control of a brain-computer interface, IEEE Trans. Neural Syst. Rehabil. Eng. 14 (2006) 246–250.
[10] T.P. Luu, S. Nakagome, Y. He, J.L. Contreras-Vidal, Real-time EEG-based brain-computer interface to a virtual avatar enhances cortical involvement in human treadmill walking, Sci. Rep. 7 (2017) 8895.
[11] G. Schalk, J. Mellinger, A Practical Guide to Brain-Computer Interfacing with BCI2000, Springer, London Dordrecht Heidelberg New York, 2010.
[12] S.R. Schultz, S. Panzeri, Temporal correlations and neural spike train entropy, Phys. Rev. Lett. 86 (2001) 5823–5826.
[13] O.A. Rosso, S. Blanco, J. Yordanova, V. Kolev, A. Figliola, M. Schürmann, E. Başar, Wavelet entropy: a new tool for analysis of short duration brain electrical signals, J. Neurosci. Methods 105 (2001) 65–75.
[14] O.A. Rosso, M.T. Martín, A. Plastino, Brain electrical activity analysis using wavelet-based informational tools, Physica A 313 (2002) (2002) 587–608.
[15] I. Osorio, M.G. Frei, Real-time detection, quantification, warning, and control of epileptic seizures: the foundations for a scientifc epileptology, Epilepsy Behav. 16 (2009) 391–396.
[16] F. Montani, A. Kohn, M.A. Smith, S.R. Schultz, The role of correlations in direction and contrast coding in the primary visual cortex, J. Neurosci. 27 (2007) 2338–2348.
[17] F. Montani, R. Ince, R. Senatore, E. Arabzadeh, M. Diamond, S. Panzeri, Phil. Trans. R. Soc. A 367 (2009) 3297–3310.
[18] F. Montani, A. Oliynyk, L. Fadiga, Superlinear summation of information in premotor neurons pairs, Int. J. Neur. Syst. 27 (2017) 1650009.
[19] O.A. Rosso, M.T. Martín, A. Figliola, K. Keller, A. Plastino, EEG analysis using wavelet-based information tools, J. Neurosci. Methods 153 (2006) 163–182.
[20] P. Goupillaud, A. Grossman, J. Morlet, Cycle-octave and related transforms in seismic signal analysis, Geoexploration 23 (1984) 85–102.
[21] O.A. Rosso, M.T. Martín, A. Plastino, Evidence of self-organization in brain electrical activity using wavelet-based informational tools, Physica A 347 (2005) 444–464.
[22] S. Blanco, A. Figliola, R. Quian Quiroga, O.A. Rosso, E. Serrano, Time-frequency analysis of electroencephalogram series. III. Wavelet packets and information cost function, Phys. Rev. E 57 (1998) 932–940.
[23] O.A. Rosso, C. Masoller, Detecting and quantifying stochastic and coherence resonances via information-theory complexity measurements, Phys. Rev. E 79 (2009) 040106(R).
[24] O.A. Rosso, C. Masoller, Detecting and quantifying temporal correlations in stochastic resonance via information theory measures, Eur. Phys. J. B 69 (2009) 37–43.
[25] G. Schalk, D.J. McFarland, T. Hinterberger, N. Birbaumer, J.R. Wolpaw, BCI2000: a general-purpose brain-computer interface (BCI) system, IEEE Trans. Biomed. Eng. 51 (2004) 1034–1043.
[26] J.R. Wolpaw, D.J. McFarland, T.M. Vaughan, G. Schalk, The Wadsworth Center brain-computer interface (BCI) research and development program, IEEE Trans. Neural Syst. Rehabil. Eng. 11 (2003) 1–4.
[27] A.L. Goldberger, L.A.N. Amaral, L. Glass, J.M. Hausdorff, P.Ch. Ivanov, R.G. Mark, J.E. Mietus, G.B. Moody, C.-K. Peng, H.E. Stanley, PhysioBank, PhysioToolkit, and PhysioNet: components of a new research resource for complex physiologic signals, Circulation 101 (23) (2000) e215–e220, https://doi.org/10.1161/01.CIR.101.23.e215, PMID: 10851218.
[28] See https://www.physionet.org/pn4/eegmmidb/ for EEG Motor Movement/Imagery Dataset.
[29] N.T.M. Huong, H.Q. Linh, L.Q. Khai, Classification of Left/Right Hand Movement EEG Signals using Event Related Potentials and Advanced Features, in: 6th IFMBE Proceedings, vol. 63, Springer, Singapore, 2018, pp. 209–215.
[30] G.F. Zebende, F.M. Oliveira Filho, J.A. Leyva Cruz, Auto-correlation in the motor/imaginary human EEG signals: A vision about the FDFA fluctuations, PLoS ONE 12 (9) (2017) e0183121.
[31] A. Belitski, A. Gretton, C. Magri, Y. Murayama, M. Montemurro, N. Logothetis, S. Panzeri, Low-frequency local field potentials and spikes in primary visual cortex convey independent visual information, J. Neurosci. 28 (2008) 5696–5709.
[32] X. Rena, Z. Yan, Z. Wang, X. Hu, Noise reduction based on ICA decomposition and wavelet transform for the extraction of motor unit action potentials, J. Neurosci. Methods 158 (2006) 313–322.
[33] P.N. Castellanos, V.A. Makarov, Recovering EEG brain signals: Artifact suppression with wavelet enhanced independent component analysis, J. Neurosci. Methods 158 (2006) 300–312.
[34] I. Daubechies, Orthonormal bases of compactly supported wavelets, Comm. Pure Appl. Math. 41 (1998) 909–996.
[35] J. Yordanova, V. Kolev, O.A. Rosso, M. Schürman, O.W. Sakowitz, M. Özgören, E. Başar, Wavelet entropy analysis of event-related potentials indicates modality-independent theta dominance, J. Neurosci. Methods 117 (2002) 99–109.
[36] O.A. Rosso, S. Blanco, A. Rabinowicz, Wavelet analysis of generalized tonic-clonic epileptic seizures, Sign Proc. 83 (2003) 1275–1289.
[37] O.A. Rosso, M.T. Martín, A. Plastino, Brain electrical activity using wavelet-based informational tools, Physica A 313 (2002) 587–608.
[38] O.A. Rosso, M.L. Mairal, Characterization of time dynamical evolution of electroencephalographic epileptic records, Physica A 312 (2002) 469–504.
[39] O.A. Rosso, Entropy changes in brain function, Int. J. Psychophys. 64 (2007) 75–80.
[40] B.A. Zeldin, P.D. Spanos, Random field representation and synthesis using wavelet bases, J. Appl. Mech. 63 (1996) 946–952.
[41] M.T. Martín, A. Plastino, O.A. Rosso, Generalized statistical complexity measures: geometrical and analytical properties, Physica A 369 (2006) 439–462.
[42] O.A. Rosso, H.A. Larrondo, M.T. Martín, A. Plastino, M.A. Fuentes, Distinguishing noise from chaos, Phys. Rev. Lett. 99 (2007) 154102.
[43] D.P. Feldman, C.S. McTague, J.P. Crutchfield, The organization of intrinsic computation: complexity-entropy diagrams and the diversity of natural information processing, Chaos 18 (2008) 043106.
[44] F. Montani, O.A. Rosso, Entropy-complexity characterization of brain development in chickens, Entropy. 16 (8) (2014) 4677–4692.
[45] F. Montani, E.B. Deleglise, O.A. Rosso, Efficiency characterization of a large neuronal network: a causal information approach, Physica A 401 (2014) 58–70.
[46] F. Montani, O.A. Rosso, F. Matias, S.L. Bressler, C.R. Mirasso, A symbolic information approach to determine anticipated and delayed synchronization in neuronal circuit models, Philos. Trans. R. Soc. Lond. Ser. A Math. Phys. Eng. Sci. 373 (2015) 20150110.

[47] F. Montani, R. Baravalle, L. Montangie, O.A. Rosso, Causal information quantification of prominent dynamical features of biological neurons, Philos. Trans. R. Soc. Lond. Ser. A Math. Phys. Eng. Sci. 373 (2015) 20150109.
[48] C. Tallon-Baudry, O. Bertrand, Oscillatory gamma activity in humans and its role in object representation, Trends Cogn. Sci. 3 (1999) 151–162.
[49] P. Hagoort, L. Hald, M. Bastiaansen, K.M. Petersson, Integration of word meaning and world knowledge in language comprehension, Science 304 (2004) 438–441.
[50] F. Olivares, A. Plastino, O.A. Rosso, Contrasting chaos with noise via local versus global information quantifiers, Phys. Lett. A 376 (2012) 1577–1583.
[51] O.A. Rosso, L. De Micco, A. Plastino, H. Larrondo, Info-quantifiers' map-characterization revisited, Physica A 389 (2010) 249–262.
[52] F. Olivares, A. Plastino, O.A. Rosso, Ambiguities in the Bandt-Pompe's methodology for local entropic quantifiers, Physica A 391 (2012) 2518–2526.
[53] A. Kowalski, M.T. Martín, A. Plastino, O.A. Rosso, Bandt-Pompe approach to the classical-quantum transition, Physica D 233 (2007) 21–31.
[54] C. Bandt, Ordinal time series analysis, Ecol. Model. 182 (2005) 229–238.
[55] O.A. Rosso, L.C. Carpi, P.M. Saco, M. Gómez Ravetti, A. Plastino, H.A. Larrondo, Causality and the entropy–complexity plane: robustness and missing ordinal patterns, Physica A 391 (2012) 42–55.
[56] O.A. Rosso, L.C. Carpi, P.M. Saco, M. Gómez Ravetti, A. Plastino, H.A. Larrondo, The Amigó paradigm of forbidden/missing patterns: a detailed analysis, Eur. Phys. J. B 85 (2012) 419.
[57] L. Zunino, M.C. Soriano, O.A. Rosso, Distinguish chaotic and stochastic dynamics from time series by using a multiscale symbolic approach, Phys. Rev. E 86 (2012) 046210.
[58] L. Zunino, M.C. Soriano, I. Fischer, O.A. Rosso, C.R. Mirasso, Permutation-information-theory approach to unveil delay dynamics from time-series analysis, Phys. Rev. E 82 (2010) 046212.
[59] M. Zanin, O.A. Rosso, L. Zunino, D. Papo, Permutation entropy and its main biomedical and econophysics applications: a review, Entropy 14 (2012) 1553–1577.